Submitted to the Editor of the Astrophysical Journal.

Electron-positron Annihilation Radiation from Sgr A East at the Galactic Center

Marco Fatuzzo[1,2], Fulvio Melia[2,3,4], and Johann Rafelski[2]

[1]Physics Department, Xavier University, Cincinnati, OH 45207

[2]Physics Department, The University of Arizona, Tucson, AZ 85721

[3]Steward Observatory, The University of Arizona, Tucson, AZ 85721

Received _____; accepted _____

[4]Sir Thomas Lyle Fellow and Miegunyah Fellow.

ABSTRACT

Maps of the Galactic electron-positron annihilation radiation show evidence for three distinct and significant features: (1) a central bulge source, (2) emission in the Galactic plane, and (3) an enhancement of emission at positive latitudes above the Galactic Center. In this paper, we explore the possibility that Sgr A East, a very prominent radio structure surrounding the Galactic nucleus, may be a significant contributer to the central bulge feature. The motivation for doing so stems from a recently proposed link between this radio object and the EGRET γ-ray source 2EG J1746-2852. If this association is correct, then Sgr A East is also expected to be a source of copious positron production. The results presented here show that indeed Sgr A East must have produced a numerically significant population of positrons, but also that most of them have not yet had sufficient time to thermalize and annihilate. As such, Sgr A East by itself does not appear to be the dominant *current* source of annihilation radiation, but it will be when the positrons have cooled sufficiently and they have become thermalized. This raises the interesting possibility that the bulge component may be due to the relics of earlier explosive events like the one that produced Sgr A East.

Subject headings: acceleration of particles—cosmic rays—Galaxy: center—galaxies: nuclei—radiation mechanisms: nonthermal—supernova remnants

1. Introduction

Electron-positron annihilation radiation from the Galactic Center region was first reported in the 1970s after the successful flight of a series of balloon-borne instruments (Johnson, Harnden & Haymes 1972; Johnson & Haymes 1973; Haymes et al. 1975). An unambiguous identification of the 511 keV line and the detection of the positronium continuum followed several years later (Leventhal, MacCallum & Stang 1978). Since that time, numerous follow-up experiments have provided additional monitoring of this source, though not always with a consistent measurement of the location or distribution of the emission, nor on the possible time variability of the 511 keV line flux (see the review by Tueller 1993). However, the Oriented Scintillation Spectrometer Experiment (OSSE) on the *Compton Gamma-Ray Observatory* was recently able to carry out high-sensitivity observations of the Galactic plane and uniquely map the distribution of positron annihilation radiation and search for time variability of the emission (Purcell et al. 1997).

The resulting maps show evidence for three distinct and significant features: (1) a central bulge source with a total flux (line plus continuum) of $\sim 3.3 \times 10^{-4}$ photons cm^{-2} s^{-1} and a Full Width at Half Maximum (FWHM) of ~ 4 degrees, (2) emission in the Galactic plane with a total flux of $\sim 10^{-3}$ photons cm^{-2} s^{-1} and a broad extension of more than 9 degrees FWHM in both latitude and longitude, and (3) an enhancement or extension of emission at positive latitudes above the Galactic Center with a total flux of $\sim 9 \times 10^{-4}$ photons cm^{-2} s^{-1} and a FWHM of over ~ 16 degrees. The average spectrum for the 1991 December viewing period of the Galactic Center (central bulge plus enhancement) exhibits a clear line feature at 509 ± 5 keV. The line width (2.5 keV) is consistent with the instrumental resolution. The observed ratio of the 511 keV line flux to the total positronium flux corresponds to a positronium fraction of 0.98 ± 0.04. In addition, OSSE found no evidence for time variability.

Sources proposed as contributers to the annihilation emission have included cosmic-ray interactions in the interstellar medium (Lingenfelter & Ramaty 1982), pulsars (Sturrock 1971) and β^+ decay products from radioactive nuclei (e.g., ^{56}Co, ^{44}Sc, and ^{26}Al) produced by supernovae, novae, or Wolf-Rayet stars (Clayton 1973; Ramaty & Lingenfelter 1979; Signore & Vedrenne 1988;

Woosley & Pinto 1988; Lingenfelter & Ramaty 1989). However, efforts to model the distribution of the 511 keV emission have been only moderately successful (see, e.g., Purcell et al. 1993). These models, consisting of components generally representing Galactic emission observed at other wavelengths (e.g., CO maps) or geometric configurations assuming that the emission of annihilation radiation follows a Galactic distribution of known sources, were not able to describe the OSSE maps adequately. It is evident that simple Galactic distributions are not sufficient to describe the most recent 511 keV data and that additional components are required. For example, the expected 511 keV line flux resulting from the radioactive decay of ^{26}Al represents only $\sim 3-9\%$ of the total Galactic 511 keV line flux (Purcell et al. 1997).

In this paper, we explore the possibility that Sgr A East, a very prominent elongated radio structure surrounding (although slightly off-centered from) the Galactic nucleus, is a significant source of the annihilation radiation associated with the bulge feature. The motivation for doing so stems from the association of this radio object and the EGRET γ-ray source 2EG J1746-2852 suggested by Melia et al. (1998). These authors show that the high-energy component of the EGRET spectrum can be accounted for by the decay of neutral pions ($\pi^0 \rightarrow \gamma\gamma$) produced in $p-p$ scatterings between ambient protons and a relativistic population accelerated by shocks within the Sgr A East shell. Since charged pions which decay leptonically ($\pi^{\pm} \rightarrow \mu^{\pm}\nu_{\mu}$, with $\mu^{\pm} \rightarrow e^{\pm}\nu_e\nu_{\mu}$) are also produced, the rest of Sgr A East's spectrum, extending down to GHz energies, is filled uniquely by the bremsstrahlung, Compton and synchrotron interactions of the associated electrons and positrons. The VLA data, for example, are consistent with the synchrotron emissivity of the decay leptons within an equipartition magnetic field of $\approx 10^{-5}$ G.

If this scenario is correct, Sgr A East must be a site of copious positron production. Here, we investigate whether this process is sufficient to power the measured flux of annihilation radiation from the Galactic Center, and if not, whether theses observations suggest an evolutionary history of Sgr A East.

The rest of the paper is organized as follows. Section 2 presents what is known about Sgr A East from observations as well as what we infer based on the results of Melia et al. (1998). This

section also includes a calculation of the ionization state of the gas in Sgr A East. The fate of positrons produced in Sgr A East is then considered in Section 3. Two different evolutionary cases for this environment are presented in Section 4. The characteristics of the annihilation radiation spectra for these cases are determined in Section 5 and compared to observations. Our concluding remarks are also given in Section 5.

2. The Environment of Sgr A East

2.1. The Basic Properties

Sgr A East is an elliptical structure with nonthermal radio emission peaked at its periphery. Geometrically, the structure is elongated along the Galactic plane with a major axis of length 10.5 pc and a center displaced from the apparent dynamical nucleus, Sgr A West, by 2.5 pc in projection toward negative Galactic latitudes. The actual distance between Sgr A West and the geometric center of Sgr A East has been estimated to be ~ 7 pc (Yusef-Zadeh & Morris 1987; Pedlar et al. 1989; Yusef-Zadeh et al. 1999). Although morphologically similar to supernova remnants (SNRs), the energetics ($\sim 4 \times 10^{52}$ ergs) of Sgr A East, based on the power required to carve out the radio synchrotron remnant within the surrounding dense molecular cloud, appear to be extreme compared to the total energy ($\sim 10^{51}$ ergs) released in a typical supernova (SN) explosion. It has been suggested that Sgr A East may be the remnant of a tidally disrupted star (Khokhlov & Melia 1996). Regardless of what actually caused the initial explosion, recent observations of this region at 1720 MHz (the transition frequency of OH maser emission) have revealed the presence of several maser spots at the SE boundary of Sgr A East with a velocity of ≈ 50 km s^{-1}, and one near the Northern arm of Sgr A West at a velocity of 134 km s^{-1} (Yusef-Zadeh et al. 1996). These observations are consistent with the presence of shocks produced at the interface between the expanding Sgr A East shell and the surrounding environment. The implied age of Sgr A East ($\tau \sim 5\,\mathrm{pc}/100$ km s$^{-1} \sim 5 \times 10^4$ yr) is then consistent with those of typical SNRs.

Given its proximity to the Galactic Center, Sgr A East is bathed by intense IR and UV radiation fields associated with the central $1 \sim 2$ parsecs of the galaxy (Telesco et al. 1998; Davidson et al. 1992; Becklin, Gatley & Werner 1982; Melia, Yusef-Zadeh & Fatuzzo 1998). Although there are no direct measurements of the properties of the ambient medium enveloped by Sgr A East, X-ray observations suggest an average electron ambient density of $\sim 3 - 6$ cm^{-3} (Koyama et al. 1996; Sidoli & Mereghetti 1999). These results are consistent with an upper limit of ~ 30 cm^{-3} inferred by Melia et al. (1998). The temperature of the ambient medium is considerably less constrained. Observationally, the ISM within the inner 150 pc is comprised of several gas components with a range of temperatures. Inside the minicavity, the electron temperature lies in the range $4000 - 7000$ K, and is comparable to the average value of 7000 K found for Sgr A West (Roberts, Yusef-Zadeh & Goss 1996). However, on a larger scale (i.e., tens of pc), the X-ray spectra observed with ASCA exhibit several emission lines from highly ionized elements that are characteristic of a ~ 10 keV thermal plasma. In particular, this region stands out in the intense 6.7 keV Kα-transition of He-like Fe (Yamauchi, et al. 1990; Koyama, et al. 1996). These spectra indicate a common origin for the plasma in the entire region, rather than a superposition of individual sources. Assuming an expansion velocity comparable to the sound speed for $kT \sim 10$ keV, Koyama et al. (1996) infer an expansion age of $\sim 10^5$ yr, which is similar to that of Sgr A East. Thus, both the X-ray plasma and the relativistic synchrotron source may have been produced by the same explosive event $\sim 0.5 - 1 \times 10^5$ yr ago. The BeppoSAX observations of the Sgr A Complex suggest somewhat different characteristics, in which the high-energy data are well fit by the sum of two thermal models with $kT \sim 0.6$ and 8 keV, with the lower temperature plasma well correlated to Sgr A East (Sidoli & Mereghetti 1999).

2.2. Other Inferred Characteristics

Adopting the scenario of Melia et al. (1998) invoked to account for the Galactic Center EGRET observations, we assume that pion-production occurs within the Sgr A East shell as a result of collisions between shock-accelerated and ambient protons (see also Markoff, Melia &

Sarcevic 1997). A crucial aspect of this mechanism is the decay of charged pions to muons, and subsequently, to relativistic electrons and positrons. The rate at which these leptons are produced is linked directly to the rate at which neutral pions are produced (since the charged pions and neutral pions are both byproducts of the same scattering events), and is therefore well constrained by the EGRET observations (Markoff, Melia & Sarcevic 1999). In addition, since the relativistic leptons radiate synchrotron emission, their energy distribution is well constrained by the radio properties of Sgr A East. These observations also provide an indirect measure of the magnetic field strength in Sgr A East (see below).

In order to keep the analysis as concise as possible while at the same time capturing the important characteristics of the Sgr A East environment, we assume a uniform and homogeneous shell geometry, with an inner radius of 4 pc and an outer radius of 5pc, and a centroid about $R = 7$ pc from the Galactic Center. The IR and UV radiation fields bathing this region are assumed to have blackbody spectra with temperatures $T_{ir} = 100$ K and $T_{uv} = 30,000$ K, respectively, and energy densities

$$u = \frac{L}{4\pi R^2 c} = 4.4 \times 10^{-10}\ \mathrm{erg\ cm^{-3}} \left(\frac{L}{2 \times 10^7\ L_\odot}\right) \left(\frac{R}{7\,\mathrm{pc}}\right)^{-2}\ , \tag{1}$$

where L is either $L_{ir} = 10^7\, L_\odot$, or $L_{uv} = 2 \times 10^7\, L_\odot$. Furthermore, we will assume that Sgr A East has an age of 75,000 years and is comprised mostly of hydrogen with an average density $n_H = 5\,\mathrm{cm^{-3}}$, and helium with an average density $n_{He} = 0.5\,\mathrm{cm^{-3}}$. The temperature profile T within the Sgr A Complex must reflect the superposition of the various components discussed above. For our purposes here, however, we assume that the ambient plasma where the positrons are produced may be ascribed a single characteristic value of T at any given time. The positrons are assumed to be produced within the Sgr A East shell in accordance with Case 2 of Melia et al. (1998), the one that produced the best fit to the gamma-ray data. The injection function I_+ for these particles is shown in Figure 1 as a function of the positron energy E_+. The total production rate, found by integrating this function over all values of E_+, is equal to 2.7×10^{-18} cm^{-3} s^{-1}. The corresponding magnetic field strength, inferred from the VLA spectrum, is $B = 1.1 \times 10^{-5}$ G, which is within a factor of 2 of its equipartition value.

One of the processes by which annihilation occurs is charge exchange between positrons and atoms. Our analysis of the electron-positron annihilation considered below will therefore require an assessment of the ionization fractions in the Sgr A East shell, which are set by the balance of total recombination and ionization rates for hydrogen and helium. For simplicity, we assume that all atoms are ionized from their ground state. We will confirm *a posteriori* that the ambient plasma in Sgr A East is highly ionized and that therefore the approximations we make here do not greatly affect the results. We can therefore ignore the trace presence of neutral helium as the charge exchange process is dominated by the more prevelant singly ionized species of this atom. In addition, the number density of ambient electrons is well-approximated by the constant value $n_e = 6\,\mathrm{cm}^{-3}$. The recombination rates are therefore independent of the ionization fractions of the species comprising the plasma, and hence the ionization equations for hydrogen and helium decouple and reduce to the following:

$$\frac{n^{HI}}{n^{HII}} = \frac{\sum_i R_{fi}^{HII}}{R_{1f}^{HI} + C_{1f}^{HI}} \,, \tag{2}$$

$$\frac{n^{HeII}}{n^{HeIII}} = \frac{\sum_i R_{fi}^{HeIII}}{R_{1f}^{HeII} + C_{1f}^{HeII}} \,, \tag{3}$$

where R_{fi} is the radiative recombination rate to state i and R_{1f} and C_{1f} are the radiative and collisional ionization rates from the ground state. Collisional recombination can be ignored for the conditions found in Sgr A East.

Since the electron self-collision rate

$$R_c \sim 1/t_c \sim 7.1 \times 10^{-10}\,\mathrm{s}^{-1}\ \ln\Lambda \left(\frac{T}{10^7\,\mathrm{K}}\right)^{-3/2} \left(\frac{n_e}{6\,\mathrm{cm}^{-3}}\right) \tag{4}$$

(Spitzer 1956) is much larger than the radiative recombination rates in the Sgr A East environment (see Figure 2), the free electrons thermalize prior to recombining. We can therefore use the collisional ionization rates for HI and HeII in terms of the ambient electron temperature T and the corresponding ground-state ionization energy χ from Bell et al. (1983). These represent the best fits to the observation and theory, and take the form

$$C_{1f} = n_e \exp(-\chi/kT)\ \ (kT/\chi)^{1/2}\ \sum_{n=0}^{5} a_n \left[\log(kT/\chi)\right]^n \,, \tag{5}$$

when $\chi/10 \leq kT \leq 10\chi$, and

$$C_{1f} = n_e(kT/\chi)^{-1/2} \left[\gamma \ln(kT/\chi) + \sum_{n=0}^{2} \beta_n (\chi/kT)^n\right] , \tag{6}$$

when $kT > 10\chi$. The values of the coefficients are given in Tables 1 and 2.

Table 1

	a_0	a_1	a_2	a_3	a_4	a_5
HI	2.3742E-08	-3.6866E-09	-1.0366E-08	-3.8010E-09	3.4159E-09	1.6834E-09
HeII	3.4356E-09	-1.6865E-09	-6.9236E-10	9.7863E-11	1.5591E-10	6.2236E-11

Table 2

	γ	β_0	β_1	β_2
HI	2.4617E-08	9.5986E-08	-9.2463E-07	3.9973E-06
HeII	3.0772E-09	1.1902E-08	-1.1514E-07	5.0489E-07

The radiative ionization rate from the ground state is given by the expression

$$R_{1f} = \int_{\chi}^{\infty} \sigma_{1f}(\epsilon) c n_\epsilon d\epsilon , \tag{7}$$

where n_ϵ is the differential number density of ionizing UV photons, normalized so that

$$\int_0^{\infty} \epsilon n_\epsilon d\epsilon = u_{uv} . \tag{8}$$

The ionization cross-section for hydrogenic atoms (e.g., HI and HeII) in their ground state is given by

$$\sigma_{1f}(\epsilon) = \frac{8h^3}{3^{3/2}\pi^2 e^2 m_e^2 c Z^2} \left(\frac{\chi}{\epsilon}\right)^3 \left[8\pi\ 3^{1/2} \left(\frac{\chi}{\epsilon}\right) \frac{e^{-4(\alpha/\beta)\cot^{-1}(\alpha/\beta)}}{1 - e^{-2\pi(\alpha/\beta)}}\right] , \tag{9}$$

where Z is the atomic number, α is the fine structure constant, $\beta = v/c$ is the ratio of the free electron speed to that of light, and the term in square brackets is an analytical expression for the gaunt factor (Spitzer 1978).

The total radiative recombination rate for hydrogenic atoms is

$$\sum_i R_{fi} = n_e \sum_i < v\sigma_{fi}(E) > , \tag{10}$$

where v and E are, respectively, the speed and kinetic energy of the electrons prior to capture,

$$\sigma_{fi}(E) = \frac{2^4}{3^{3/2}} \frac{he^2}{m_e^2 c^3} \frac{\chi^2}{(E + \chi/i^2)E} \frac{g}{i^3} \tag{11}$$

is the cross-section for radiative capture to the i-th state, and the brackets <> denote an average over the thermal electron distribution function. The sum over i may be truncated at $i = 20$ without introducing any appreciable error. For simplicity, the gaunt factors g are set equal to unity, therefore introducing a possible error that ranges from $\sim 3\%$ at $T = 10^4$ K to $\sim 20\%$ at temperatures in excess of 10^6 K. We note, however, that our final results are not subject to the large errors incurred at temperatures $\geq 10^6$ K.

Values of the rate coefficients as a function of the ambient temperature T are shown in Figure 2. Note that the radiative recombination rates are lower at all temperatures than the electron self-collision rate, as discussed above. For these conditions then, the ionization equations are easily solved to determine the atomic number densities. The results of these calculations are shown in Figure 3, and these help to justify the assumption stated earlier that the plasma is highly ionized for the environment in the Sgr A East shell.

3. The Positron Population

In this section, we calculate the positron distribution, and determine whether these particles thermalize before annihilating. We then consider how to calculate the present positron number density for a given evolution of the Sgr A East environment.

3.1. The Positron Annihilation Rates

Positron annihilation in a hydrogen and helium plasma can occur via three dominant mechanisms: direct (in-flight) annihilation; radiative capture; and charge exchange. The first of these processes, in which a free positron annihilates with an ambient electron without first forming positronium, results in the production of two photons. The direct annihilation rate for a positron

of kinetic energy E_+ interacting with an isotropic Maxwell-Boltzman distribution $n_e f_{mb}(E_-)$ of electrons (where E_- is the electron kinetic energy) is given by the expression

$$R_{da}(E_+) = cn_e \int f_{mb}(E_-)dE_- \int_{-1}^{1} \frac{d\mu}{2} f_{kin}(E_+, E_-)\, \sigma_{da}(E_+, E_-)\,, \tag{12}$$

where

$$f_{kin} = \left[\beta_-^2 + \beta_+^2 - \beta_-^2\beta_+^2\,(1-\mu^2) - 2\beta_-\beta_+\mu\right]^{1/2} \tag{13}$$

accounts for the kinematics of the two-particle motion, and

$$\beta_\pm = \left[\frac{2E_\pm m_e c^2 + E_\pm^2}{(mc^2)^2 + 2E_\pm m_e c^2 + E_\pm^2}\right]^{1/2} \tag{14}$$

are the positron/electron speeds in units of c. The cross-section as a function of the relative Lorentz factor $\gamma = (1-\beta^2)^{-1}$ can be determined using the plane-wave approximation and is found to be

$$\sigma_{da} = \left[2\pi\left(\frac{\alpha}{\beta}\right)\left(1 - e^{-2\pi\alpha/\beta}\right)^{-1}\right]\left[\frac{\pi r_0^2}{\gamma+1}\left(\frac{\gamma^2+4\gamma+1}{\gamma^2-1}\ln[\gamma + (\gamma^2-1)^{1/2}] - \frac{\gamma+3}{(\gamma^2-1)^{1/2}}\right)\right]\,, \tag{15}$$

where

$$\beta = \left[\frac{(1-\beta_+\beta_-\mu)^2 - (1-\beta_+^2)(1-\beta_-^2)}{(1-\beta_+\beta_-\mu)^2}\right]^{1/2} \tag{16}$$

is the relative speed (in units of c) between the electrons and positrons (Coppi & Blandford 1990), r_0 is the classical electron radius, and the term in the first set of square brackets takes into account the Coulomb attraction.

Radiative capture produces positronium in either a singlet spin-0 state (0.25 probability) or a triplet spin-1 state (0.75 probability). Annihilation from the singlet state produces two line photons whereas annihilation from the triplet state produces three continuum photons. The overall capture rate is given by summing over the radiative capture rates into each state i:

$$R_{rc}(E^+) = \sum_i c\, n_e \int f_{mb}(E_-)dE_- \int_{-1}^{1} \frac{d\mu}{2} f_{kin}(E_+, E_-)\, \sigma_{rc}(E_+, E_-)\,, \tag{17}$$

where the cross-section is easily generalized from Equation (11) by replacing m_e with the reduced mass $m_e/2$ and noting that the ionization energy from the ground state of positronium is $\chi = 6.8$ eV.

The presence of HeII implies that charge exhange (e^+ + HeII → Ps + HeIII) is an important mechanism by which positronium is formed. The rate at which this process occurs is given by

$$R_{ce}(E_+) = n_{HeII}\ \beta_+ c\sigma_{ce}(E_+)\ . \tag{18}$$

To our knowledge, no generally accepted theoretical or experimental value exists for the cross-section of this process. However, based on measurements of the cross-sections for the e^+ + HI → Ps + HII (Sperber et al. 1992) and the e^+ + HeI → Ps + HeII reactions (Overton et al. 1993), it is clear that the desired cross-section is peaked at 54.4 eV (the ground-state ionization energy for HeII) with a value there of $\sim \pi a_0^2$. Assuming an energy profile similar to that of the e^+ + HeI → Ps + HeII cross-section, we may therefore adopt an empirically based cross-section of the form

$$\sigma_{ce}(E_+) = 2.4 \times 10^{-16}\ \mathrm{cm}^2\ \left(\frac{E_+}{E_1} - 1\right)\ e^{\left(1-\frac{E_+}{E_1}\right)}\ , \tag{19}$$

for positron kinetic energies $E_+ > E_1 = 28$ eV.

The annihilation rates are shown as functions of the positron kinetic energy in Figures 4-6 for three different values of the ambient temperature. The dotted lines, which represent the Maxwell-Boltzman functions $f_{mb}(E_-)$ at each specified temperature, will be introduced in § 4.

3.2. The Positron Cooling Rates

We present here the cooling rates for a positron moving through Sgr A East with a Lorentz factor $\gamma_+ = [1 - \beta_+^2]^{-1}$. The dominant energy loss mechanisms are: (1) Synchrotron losses at a rate

$$\frac{dE_s}{dt} = -\frac{4}{3}\frac{\sigma_T c}{8\pi}\beta_+^2\gamma_+^2 B^2\ ; \tag{20}$$

(2) Compton scattering losses at a rate

$$\frac{dE_\gamma}{dt} = -\frac{4}{3}m_e c^3\beta_+^2\gamma_+^2\left[\frac{u_{uv}\sigma_c\left(x_{uv}\right)}{m_e c^2 + \gamma_+ kT_{uv}} + \frac{u_{ir}\sigma_c\left(x_{ir}\right)}{m_e c^2 + \gamma_+ kT_{ir}}\right]\ , \tag{21}$$

where $x_{uv} = 2.7\gamma_+ kT_{uv}/m_e c^2$, $x_{ir} = 2.7\gamma_+ kT_{ir}/m_e c^2$, and

$$\sigma_c(x) = \frac{3}{4}\sigma_T\left[\frac{1+x}{x^3}\left(\frac{2x(1+x)}{1+2x} - \ln(1+2x)\right) + \frac{1}{2x}\ln(1+2x) - \frac{1+3x}{(1+2x)^2}\right]\ ; \tag{22}$$

(3) Bremmstrahlung emission losses at a rate

$$\frac{dE_B}{dt} = -4\alpha r_o^2 m_e c^3 (2n_H + 6n_{He}) \ln(2\gamma_+ - 1/3)\gamma_+ \; ; \tag{23}$$

and (4) Coulomb losses at a rate of

$$\frac{dE_C}{dt} = -m_e c^3 n_e \int f_{mb}(E^-) dE^- \int_{-1}^{1} \frac{d\mu}{2} \, f_{kin} < \sigma\Delta\gamma > \, , \tag{24}$$

where

$$< \sigma\Delta\gamma >= \frac{3\sigma_T(\gamma_- - \gamma_+)}{64\epsilon^2} \left[(4\ln\Lambda + 4\ln 2) \left(\frac{\epsilon^2 + p^2}{p^2} \right)^2 - 2\left(\frac{8\epsilon^4 - 1}{p^2\epsilon^2} \right) + \frac{12\epsilon^4 + 1}{\epsilon^4} - \frac{8p^2}{3} \frac{(\epsilon^2 + p^2)}{\epsilon^4} + \frac{2p^4}{\epsilon^4} \right] \tag{25}$$

is given in terms of the parameters $\epsilon^2 = (1 + \gamma)/2$ and $p^2 = \epsilon^2 - 1$, where γ is the relative Lorentz factor (Coppi and Blandford 1990). The corresponding cooling rates, defined by the general expression $R = E_+^{-1}(dE/dt)$, are plotted in Figure 7 for an ambient temperature of 10^5 K. We note that only the Coulomb cooling rate depends on the temperature, with the low-energy turnover occuring at an energy of $\sim kT$.

3.3. The Fate of Positrons in Sgr A East

It is clear from the results shown in Figures 4-7 that the total positron cooling rate is much greater than the total positron annihilation rate over the entire energy range. In addition, for energies below $\sim 10^8$ eV, the total cooling rate increases with decreasing particle energy. Taken together, these results imply that particles produced in Sgr A East with energies $\leq 10^8$ eV thermalize to the same temperature as the ambient electrons on a time scale equal to the inverse of their initial cooling rate, and do so before they annihilate. These results are summarized in Figure 8, which shows the total annihilation (short-dash) and cooling (long-dash) rates assuming an ambient temperature of $T = 10^5$ K along with the injection function (solid line, right-hand scale) for the Sgr A East positrons. The two horizontal dotted lines mark the inverse of 10^4 and 10^5 years, and the energy at which they first intersect the injection function then yields the threshold energy below which particles (i.e., those to the left of the corresponding vertical lines)

have had sufficient time to thermalize within that time scale. A plot of the threshold energy E_t as a function of time ranging between 10^4 and 10^5 years is shown in Figure 9. Figure 10 then illustrates the rate per unit volume with which positrons thermalize in Sgr A East (found by integrating the injection function up to the threshold energy) as a function of its age. This value falls well short of the total rate per unit volume with which positrons are produced in Sgr A East (2.7×10^{-18} cm^{-3} s^{-1}) since E_t is smaller than the energy at the peak of the injection function.

In other words, Sgr A East is apparently producing positrons at a rate that is currently much higher than that with which they cool and thermalize. The positrons in this remnant are being "stockpiled."

4. Evolutionary Models of Sgr A East

The number density of *thermal* positrons populating Sgr A East as a function of its age t^* is found by integrating the evolution equation

$$\frac{dn_+}{dt} = \left[\int_0^{E_t(t^*)} I_+(E)dE\right] - \left[n_+ \left(< R_{da} > + < R_{ce} > + < R_{rc} >\right)\right] \ , \tag{26}$$

where I_+ is the injection function shown in Figure 1 and the terms in the <> brackets represent the annihilation rates (da - direct annihilation; ce - charge exchange; rc - radiative capture) averaged over the thermal positron distribution function. Note that the term in the first square brackets represents the rate at which positrons are thermalized in Sgr A East.

We first consider a static evolutionary model for Sgr A East where both the temperature and thermalization rate are constant in time. For this case, the number density of positrons increases with age until the annihilation rate matches the thermalization rate. Assuming that all thermal positrons form positronium before annihilating, each positron produces an average of $0.25 \times 2 + 0.75 \times 3 = 2.75$ annihilation photons. A reasonably good estimate for the ensuing flux at Earth, found by multiplying the product of the injection rate (which is clearly larger than the thermalization/annihilation rate) and the Sgr A East volume by 2.75 to find the total rate of annihilation radiation photons produced in Sgr A East, and then dividing by $4\pi D^2$ (where

$D = 8.5$ kpc is the distance to the Galactic Center), yields a value of $6.5 \times 10^{-6}\,\mathrm{cm}^{-2}\ \mathrm{s}^{-1}$. This number is clearly much smaller than the measured flux arriving at earth from the bulge.

Is it possible then that a time-dependent positron production rate in Sgr A East could account for the current high rate of annihilation? Let us consider the possibility that positrons were stockpiled in Sgr A East during its infancy, and are now being depleted at a rate exceeding the current thermalization rate. This feat can be accomplished in two ways. First, the positron injection rate in Sgr A East may have been much higher earlier in its life. Indeed, the energy content of the relativistic proton population for Case 1 of Melia et al. (1989) is 7.7×10^{51} ergs, or roughly 10% of the energy associated with Sgr A East. (We note, however, that this value is really an upper limit, as it was derived assuming steady state conditions.) In that case, the number density of positrons populating Sgr A East would now be $\sim 10^{-2}$ cm^{-3}. In contrast, for the static evolutionary model discussed above, the number density of positrons injected into Sgr A East during the assumed lifetime of 75,000 years is $\sim 6 \times 10^{-6}$ cm^{-3}. This difference suggests that the initial injection rate may have been as high as 10^4 times greater than what is observed today.

We therefore consider two cases for the evolution of the injection rate, both of the form

$$I_+(t) = A\, I_+(t^*) \exp(-t/\tau)\ , \tag{27}$$

where $A = 10^2$ for Case A and $A = 10^4$ for Case B. The value for τ is then well-defined for the assumed age t^* of 75,000 years.

Another reason why positrons may have been stockpiled in Sgr A East is that its temperature decreases with age. This can be seen by considering the annihilation rates averaged over the thermal positron distribution as a function of temperature. As shown in Figure 11, the averaged charge-exchange rate is strongly peaked at $\sim 10^5$ K, where the overlap between the Maxwell-Boltzman distribution function and the charge-exchange rate produces a clear maximum (see Figures 4 - 6). It is intriguing that the lower limit of 0.94 for the positronium fraction observed from the Galactic Center indicates that the temperature where the annihilation radiation is produced must lie in the range between 3.2×10^4 K and 3.2×10^5 K. This result is clearly seen

from the plot of the positronium fraction

$$f_{Ps} = \frac{< R_{ce} > + < R_{rc} >}{< R_{ce} > + < R_{rc} > + < R_{da} >} \tag{28}$$

versus temperature, as shown in Figure 12. These results are somewhat consistent with the observed line-width of 2.5 keV, since the expected relation

$$\frac{\Delta\epsilon}{\epsilon} \approx 3.2 \times 10^{-3} \left(\frac{T}{10^4\,\mathrm{K}}\right)^{0.41} , \tag{29}$$

(Wallyn et al. 1996) then implies a temperature of $\approx 2.8 \times 10^4$ K. We caution, however, that the above line-width relation is somewhat suspect (as noted by Wallyn et al.). We therefore assume that the initial temperature of Sgr A East may have been 10^7 K and that it decays exponentially so that the temperature will be 10^5K at an age of 10^5 years.

5. Results and Discusson

We have integrated Equation (26) for the two evolutionary cases (A and B) discussed above. The number densites as a function of age for these situations are shown in Figure 13 as solid lines. The dotted lines represent the number densities stockpiled in the event that the annihilation rates are zero. To gain insight into these results, we plot the rate per unit volume at which positrons are thermalized (dotted line) and annihilated (solid and dashed lines) as a function of age for case B in Figure 14. It is clear that the positrons are indeed stockpiled when the thermalization rates are high, and this stockpile is depleted when the charge-exchange annihilation rate peaks.

The ensuing annihation spectrum is easily determined by noting that the observed flux of line photons is given by

$$F_l = \frac{N_+}{4\pi D^2} \left(2 < R_{da} > +0.5 < R_{rc} > +0.5 < R_{ce} >\right) , \tag{30}$$

and the observed flux of continuum photons is given by

$$F_c = \frac{N_+}{4\pi\ D^2} \left(2.25 < R_{rc} > +2.25 < R_{ce} >\right) , \tag{31}$$

where N_+ is the total number of thermal positrons in Sgr A East. The total flux observed as a function of age is presented in Figure 15 for the two cases discussed above. As expected, the flux peaks at around $75,000$ years, where the positrons are just beginning to be depleted.

It is clear by comparing the values in Figure 15 to the observed flux from the bulge that even ideal evolutionary conditions cannot make up for the fact that only a small fraction of the injected positrons will have thermalized and are annihilating. This point is emphasized by the requirement of a very efficient cooling mechanism for the conditions in Sgr A East to account for the observed annihilation radiation flux, as may be seen by making the *ad hoc* assumption that all of the injected positrons thermalize. In that (extreme) case, the resulting flux curve (as shown in Figure 16 for the case with $A = 10^2$) would agree well with the observations.

Our first conclusion is therefore that Sgr A East is not (by itself) the source of annihilation radiation from the Galactic Center, unless some efficient cooling mechanism (not considered here) is thermalizing the positrons on a time scale shorter than the age of this remnant.

However, since Sgr A East's age is much shorter than the age of the Galaxy, it is reasonable to ask whether the process that produced this relatively unique remnant was a singular event. If not, then the accumulated "stockpiles" of positrons may now be at the required level to account for the observed annihilation rate. Unfortunately, there is very little to go by in terms of phenomenologically pinning down the rate at which these explosive events have occurred. But we can at least use the properties of the bulge component of the e^+e^- annihilation radiation to infer what the minimum explosion rate must have been.

Using the required positron density, and assuming that no special cooling rate, beyond what we have considered here, is acting on the positrons, we estimate that ~ 30 explosions (like the one that produced Sgr A East) must have occurred over the past one million years if $A = 10^2$. The number of events drops as the value of A increases, reaching about one event per million years when $A = 10^4$. This is interesting in view of the fact that Sgr A East's age is estimated to be about 75,000 years, which means that indeed we may be witnessing the most recent of a series of catastrophic events that occur on average about once every 30,000 to 1 million years. This lends

indirect support to the idea (Khokhlov and Melia 1996) that Sgr A East may have been produced by the tidal disruption of a $\sim 2\ M_\odot$ star that ventured within 10 Schwarzschild radii or so of the central black hole. Given the stellar density in the vicinity of Sgr A*, such events are expected to occur roughly once every 10,000 to 100,000 years. The bulge component of the e^+e^- annihilation radiation may therefore be the best evidence we have right now for the existence of accumulated relics of this ongoing stellar disruption process.

Acknowledgments This research was partially supported by NASA under grants NAG5-8239 and NAG5-9205, and has made use of NASA's Astrophysics Data System Abstract Service. FM is very grateful to the University of Melbourne for its support (through a Miegunyah Fellowship) and MF would like to thank the John Hauck Foundation for partial support.

REFERENCES

Becklin, E.E., Gatley, I., & Werner, M.W. 1982, *ApJ*, **258**, 134.

Bell, K.L, Gilbody, H.B., Hughes, J.G., Kingston, A.E., & Smith, F.J. 1983, J. Phys. Chem. Ref. Data, **12**, 891

Clayton, D.D. 1973, Nature Phys. Sci., **244**, 137.

Coppi, P.S. & Blandford, R.d. 1990, MNRAS, **245**, 453.

Davidson, J.A. et al. 1992, *ApJ*, **387**, 189.

Haymes, R.C., Walraven, G.D., Meegan, C.A., Hall, R.D., Djuth, F.T., & Shelton, D.H. 1975, *ApJ*, **201**, 593.

Johnson, W.N., Harnden, F.R. Jr. & Haymes, R.C. 1972, *ApJ (Letters)*, **172**, L1.

Johnson, W.N. & Haymes, R.C. 1973, *ApJ*, **184**, 103.

Khokhlov, A. & Melia, F. 1996, *ApJ (Letters)*, **457**, 61.

Koyama, K., Maeda, Y., Sonobe, T., et al. 1996, PASJ, **48**, 249.

Leventhal, M., MacCallum, C.J. & Stang, P.D. 1978, *ApJ (Letters)*, **225**, L11.

Lingenfelter, R.E. & Ramaty, R. 1982, The Galactic Center, ed. G.R. Riegler & R.D. Blandford (New York: AIP), 148.

Lingenfelter, R.E. & Ramaty, R. 1989, *ApJ*, **343**, 686.

Markoff, S., Melia, F. & Sarcevic, I. 1997, *ApJ (Letters)*, **489**, 47.

Markoff, S., Melia, F. & Sarceivc, I. 1999, *ApJ*, **522**, 870.

Melia, F., Fatuzzo, M., Yusef-Zadeh, F. & Markoff, S. 1998, *ApJ (Letters)*, **508**, L65.

Melia, F., Yusef-Zadeh, F., & Fatuzzo, M. 1998, *ApJ*, **508**, 676.

Overton, N., Mills, R.J., & Coleman, P.J. 1993, J. Phys. B., **25**, 557

Pedlar, A., et al. 1989, *ApJ*, **342**, 769.

Purcell, W.R. et al. 1993, *ApJ (Letters)*, **413**, L85.

Purcell, W.R. et al. 1997, *ApJ*, **491**, 725.

Ramaty, R. & Lingenfelter, R.E. 1979, *Nature*, **278**, 127.

Roberts, D.A., Yusef-Zadeh, F. & Goss, W.M. 1996, *ApJ*, **459**, 627.

Sidoli, L. & Mereghetti, S. 1999, A&A *(Letters)*, **349**, L49.

Signore, M. & Vedrenne, G. 1988, A&A, **201**, 379.

Sperber, W., et al. 1992, Phys. Rev. Lett., **68**, 3690

Spitzer, L. 1956, Physics of Fully Ionized Gases (Interscience Publishers, New York).

Spitzer, L. 1978, Physical Processes in the Interstellar Medium (John Wiley & Sons, New York).

Sturrock, P.A. 1971, *ApJ*, **164**, 529.

Telesco, C.M., Davidson, J.A. & Werner, M.W. 1996, *ApJ*, **456**, 541.

Tueller, J. 1993, Proc. Compton Symp., ed. M. Friedlander & N. Gehrels (New York: AIP), 97.

Wallyn, P., Mahoney, W.A., Durouchoux, PH., & Chapuis, C. 1996, *ApJ*, **465**, 473.

Woosley, S.E. & Pinto, P.E. 1988, Nuclear Spectroscopy of Astrophysical Sources, ed. N. Gehrels & G.H. Share (New York: AIP), 98.

Yamauchi, S., Kawada, M., Koyama, K., et al. 1990, *ApJ*, **365**, 532.

Yusef-Zadeh, F. & Morris, M. 1987, *ApJ*, **320**, 545.

Yusef-Zadeh, F., Roberts, D. A., Goss, W. M., Frail, D. A. & Green, A. J. 1996, *ApJ (Letters)*, **466**, L25.

Yusef-Zadeh, F., Roberts, D. A., Goss, W. M., Frail, D. A. & Green, A. J. 1999, *ApJ*, **527**, 172.

This manuscript was prepared with the AAS LaTeX macros v4.0.

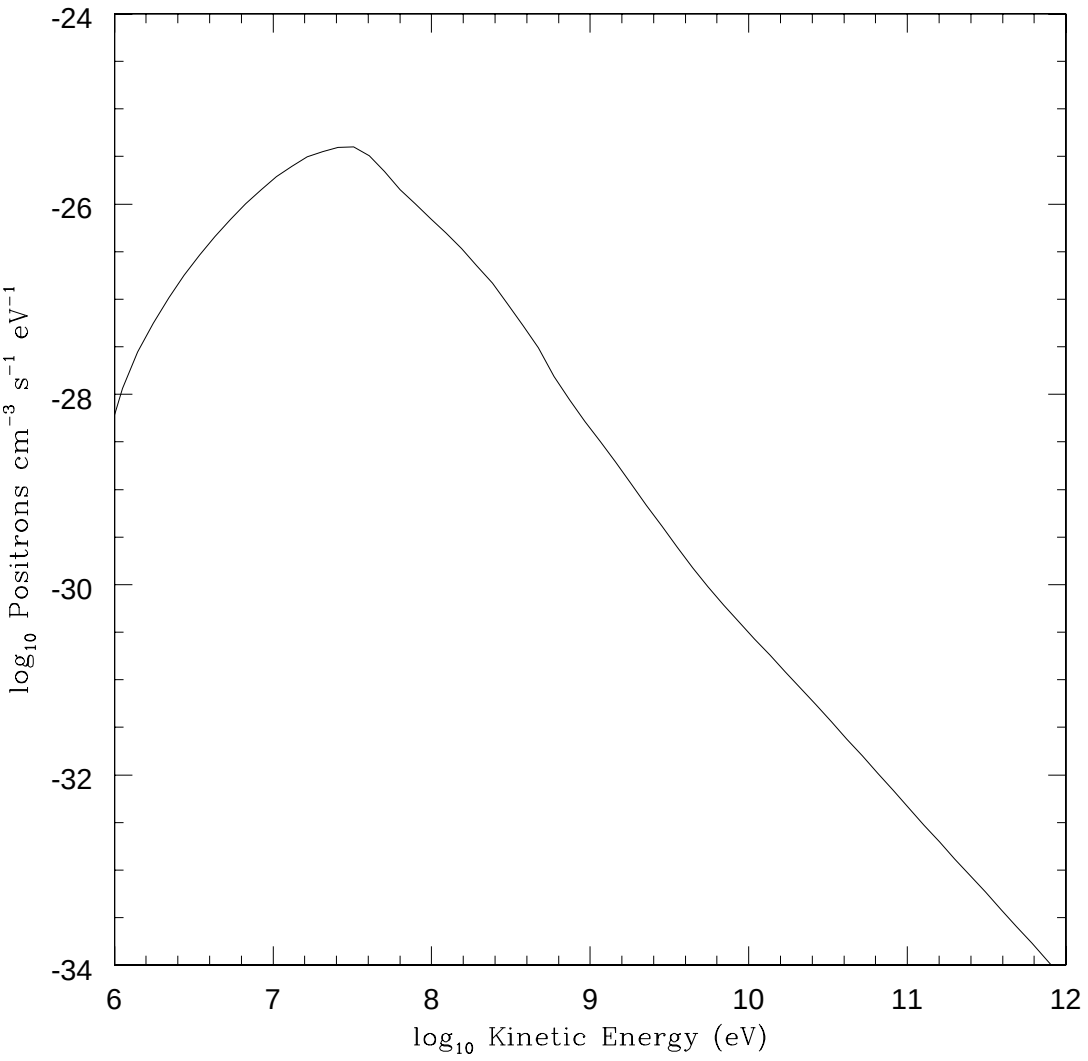

Fig. 1.— The injection function $I_+(E_+)$ for positrons produced via charged pion decay in Sgr A East, assuming conditions adopted in Case 2 of Melia et al. (1998). The total rate per unit volume at which positrons are produced, determined by integrating this function over the positron kinetic energy, is equal to 2.7×10^{-18} cm^{-3} s^{-1}.

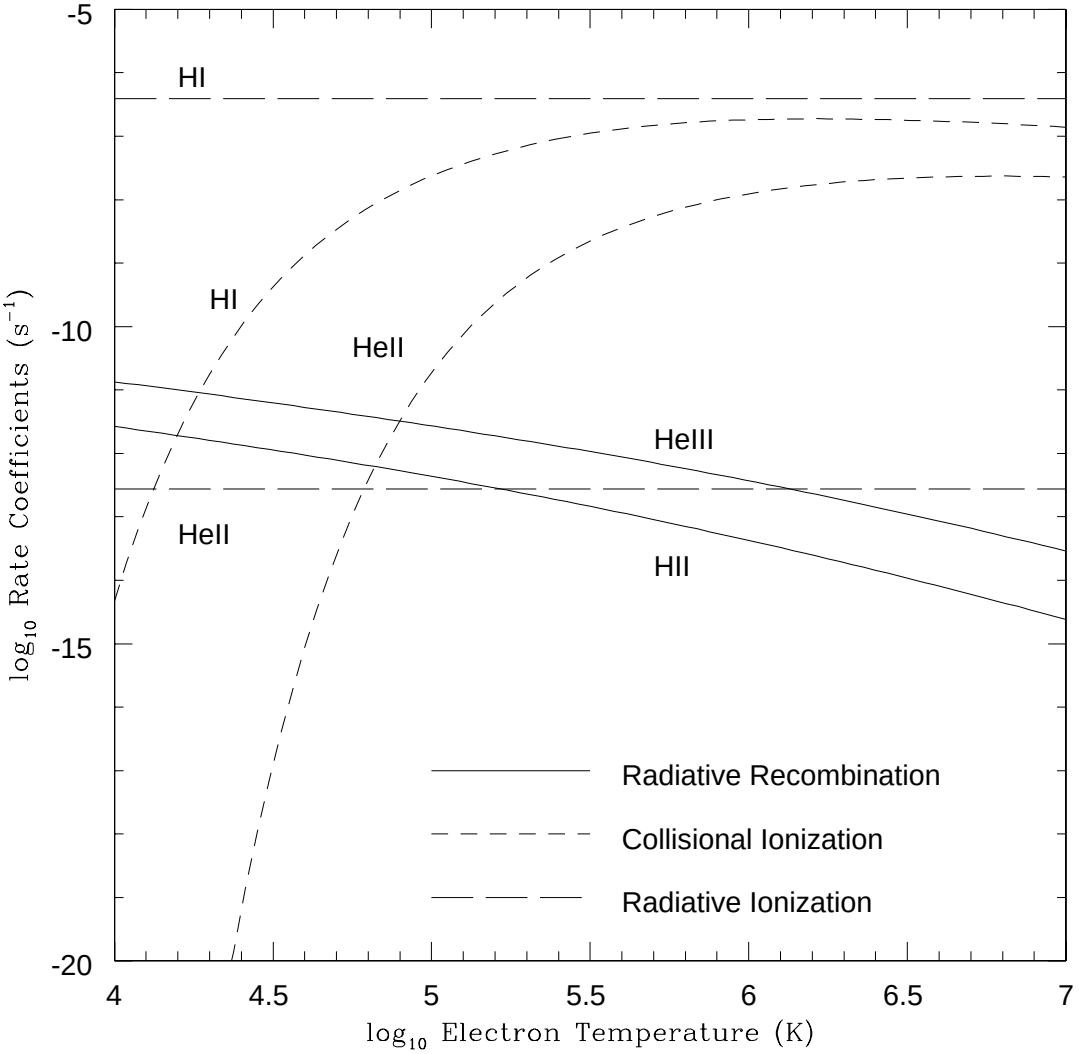

Fig. 2.— Recombination and ionization rates for hydrogen and helium in Sgr A East as a function of the ambient electron temperature.

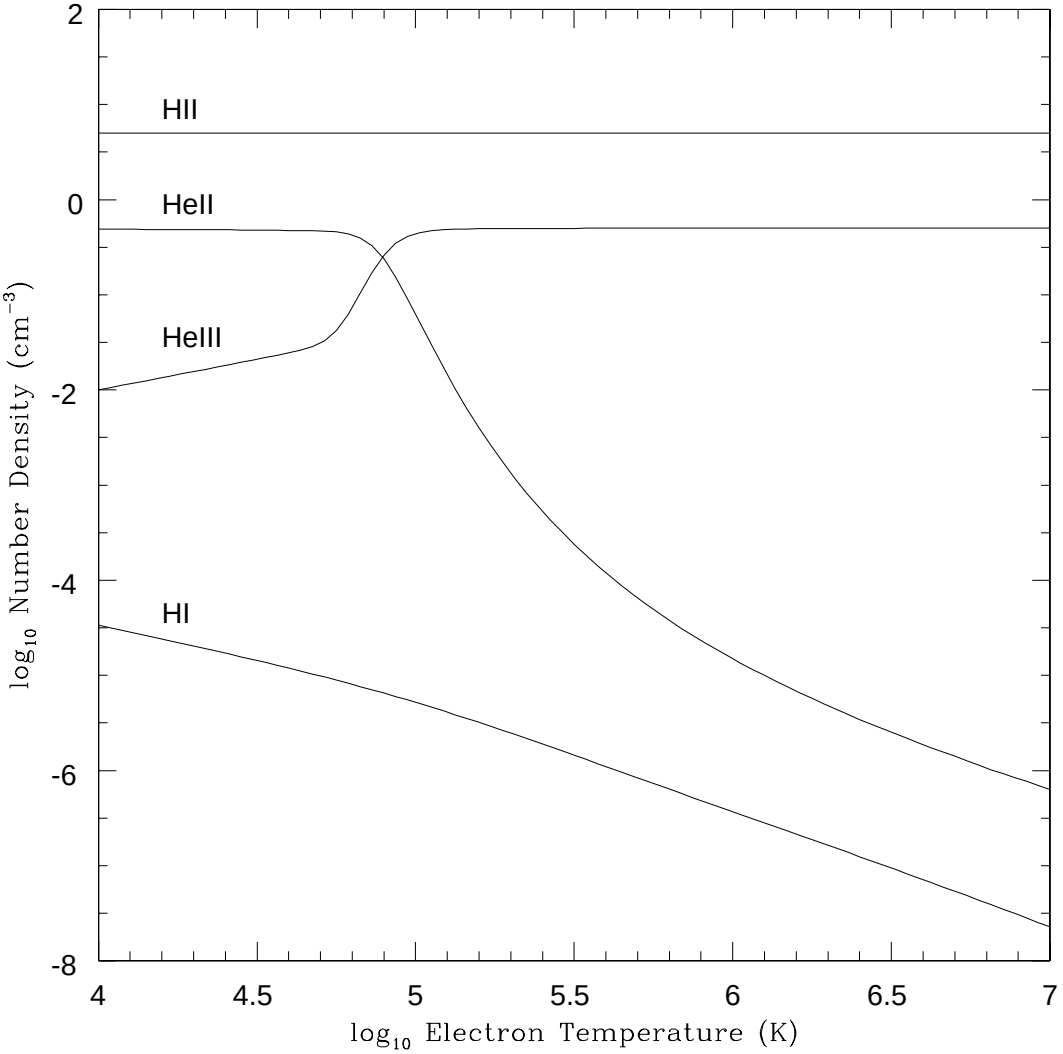

Fig. 3.— The number density of neutral and ionized hydrogen and of singly and doubly ionized helium in Sgr A East as a function of the ambient electron temperature.

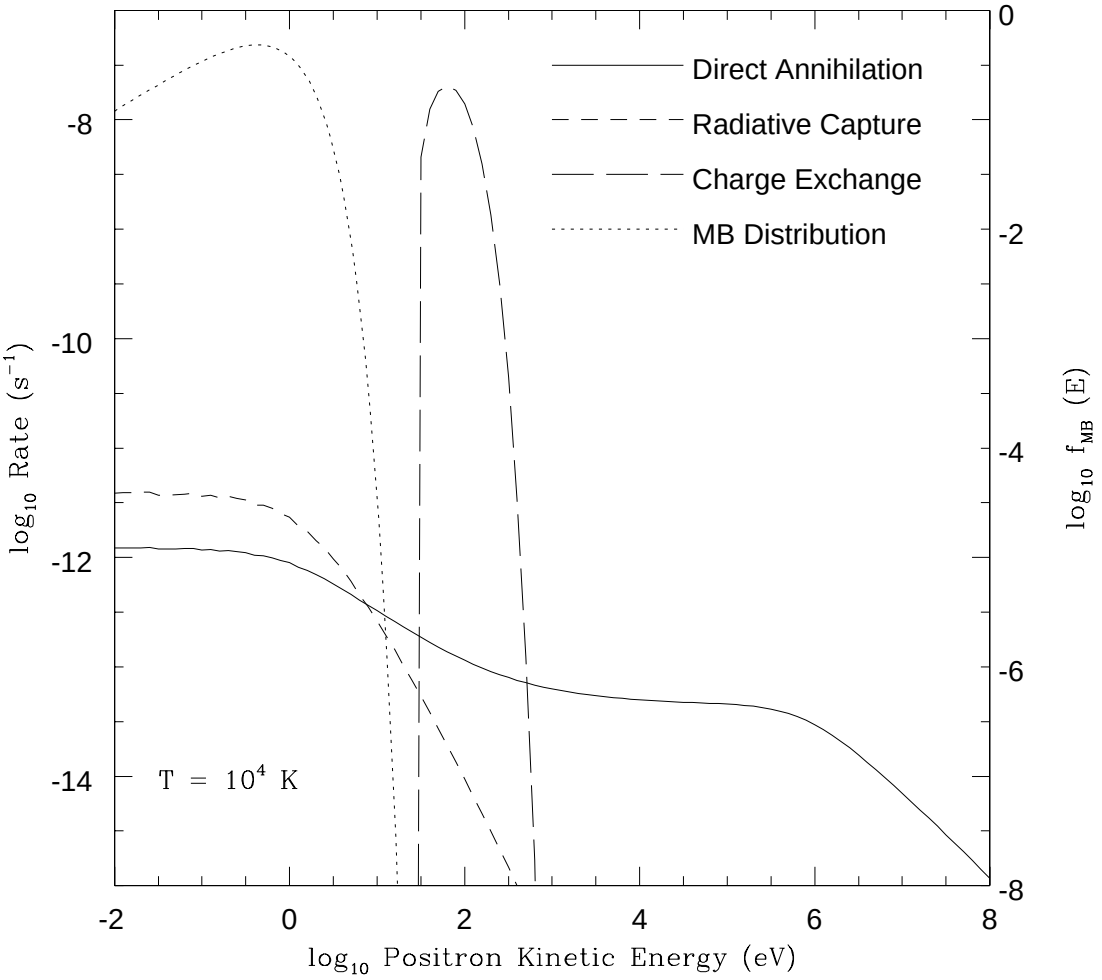

Fig. 4.— Annihilation rates as a function of positron kinetic energy for an ambient temperature of 10^4 K.

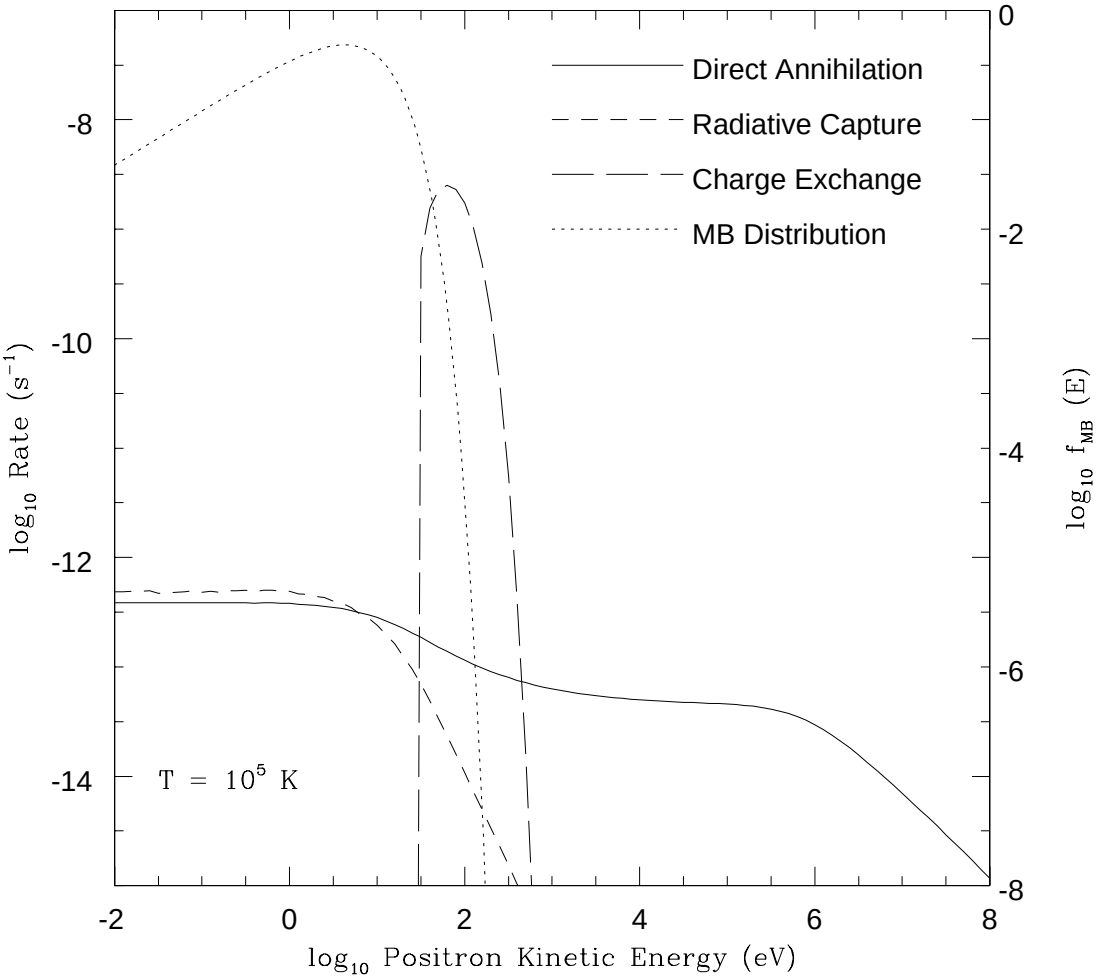

Fig. 5.— Annihilation rates as a function of positron kinetic energy for an ambient temperature of 10^5 K.

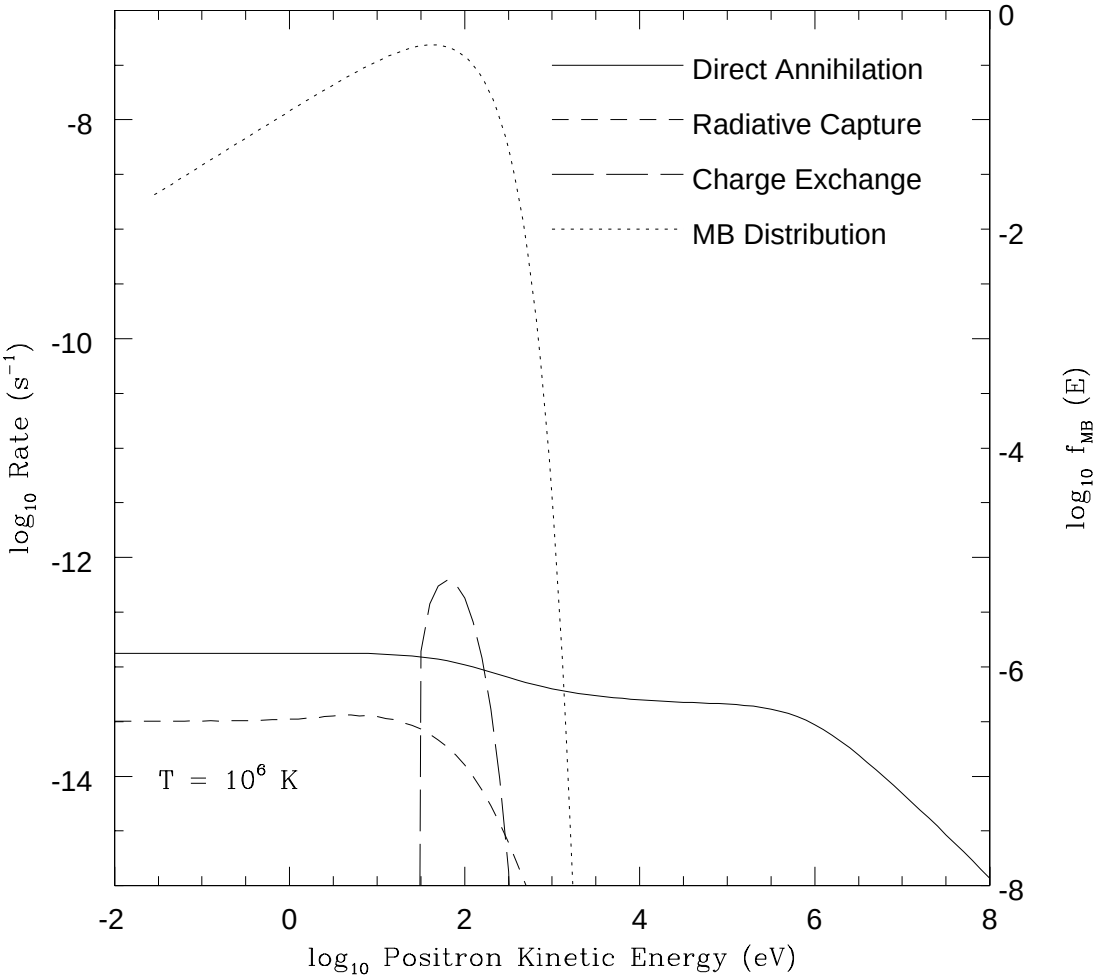

Fig. 6.— Annihilation rates as a function of positron kinetic energy for an ambient temperature of 10^6 K.

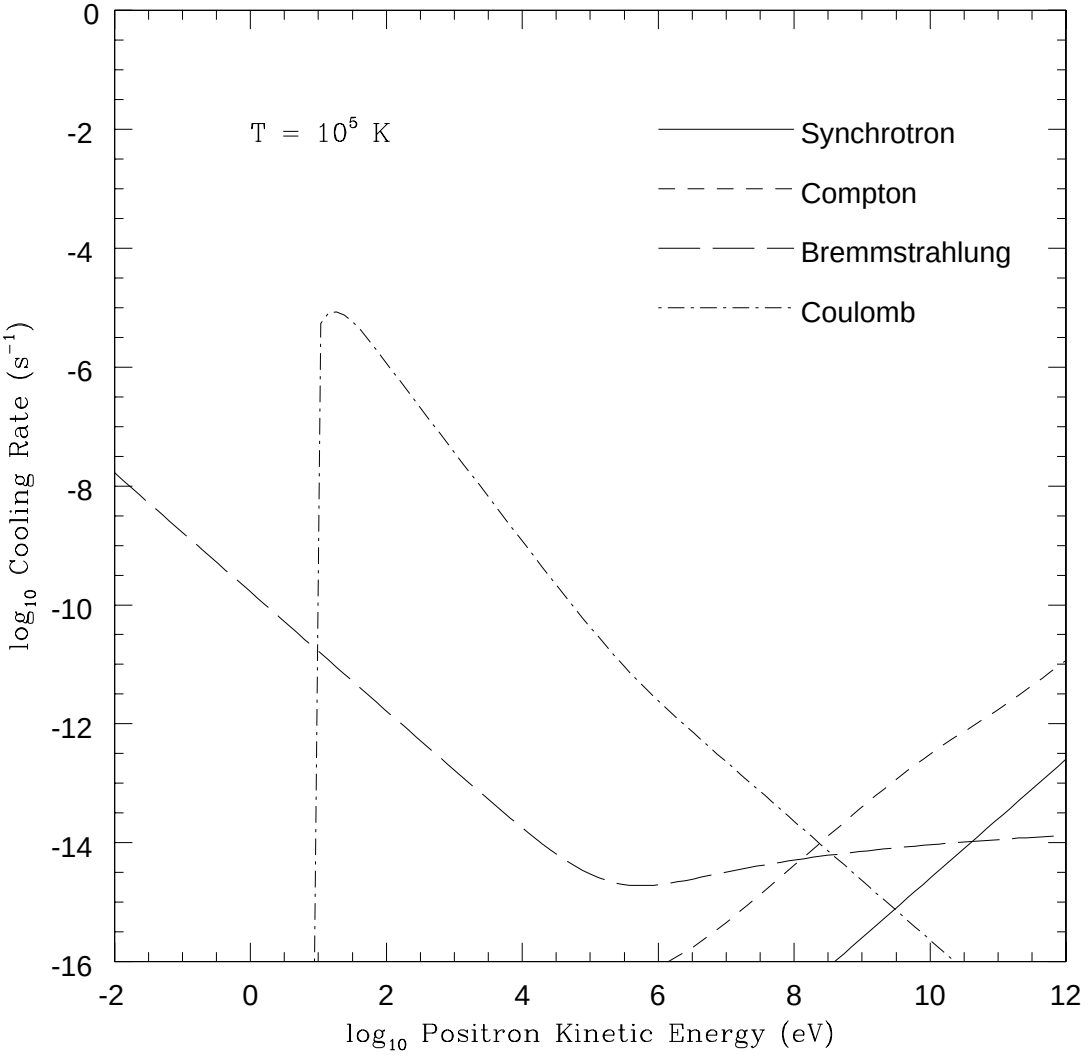

Fig. 7.— Cooling rates as a function of positron kinetic energy for an ambient temperature of 10^5 K.

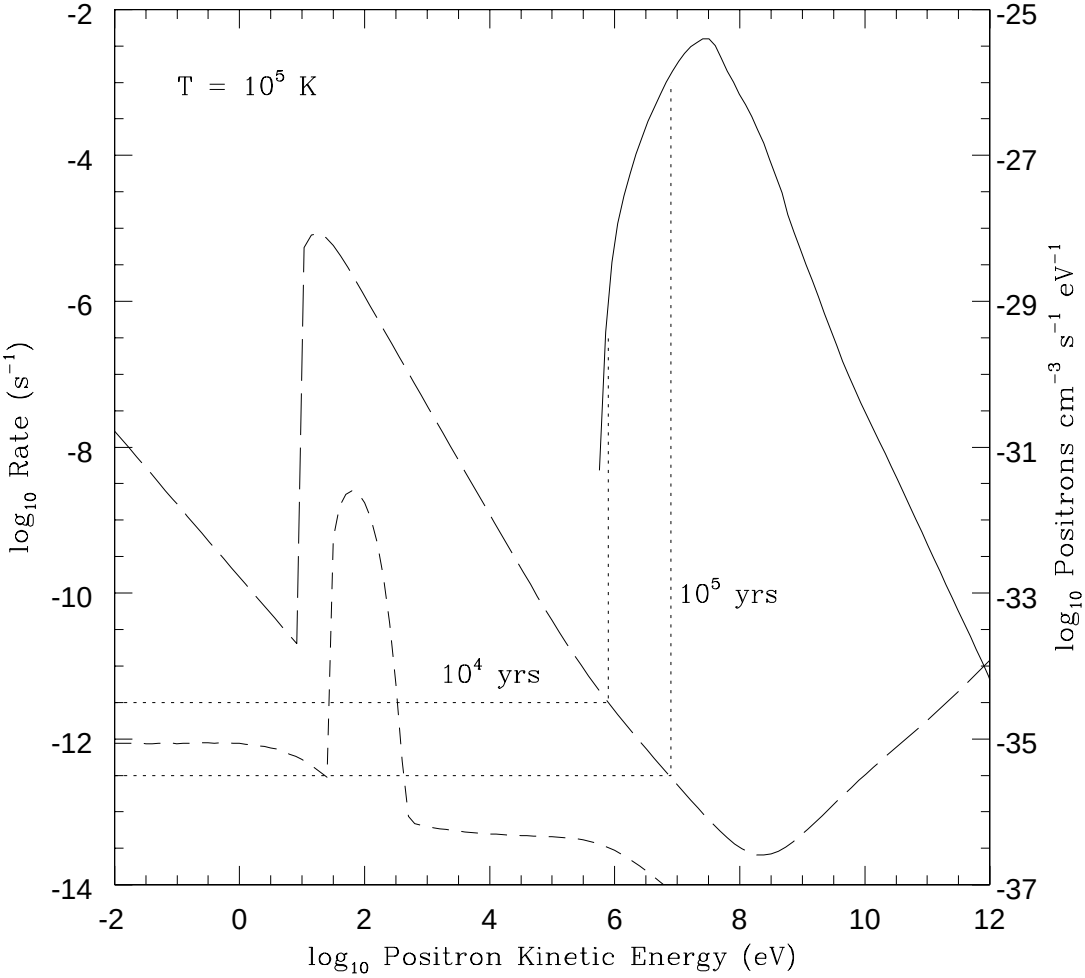

Fig. 8.— A direct comparison between the total annihilation and cooling rates, and the injection function in terms of the positron kinetic energy for an ambient temperature of 10^5 K.

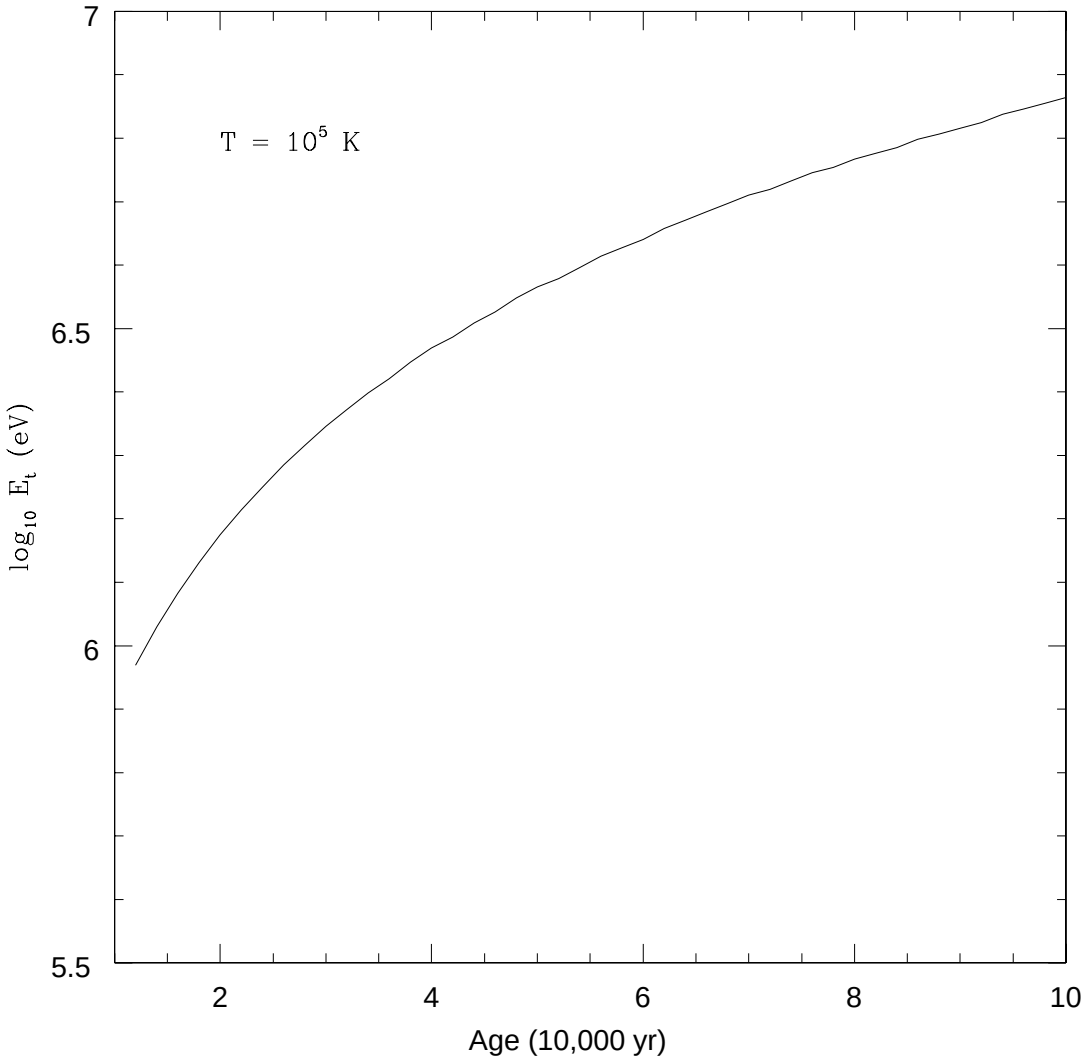

Fig. 9.— The threshold energy below which positrons thermalize on a time scale shorter than the age of Sgr A East as a function of the remnant's age.

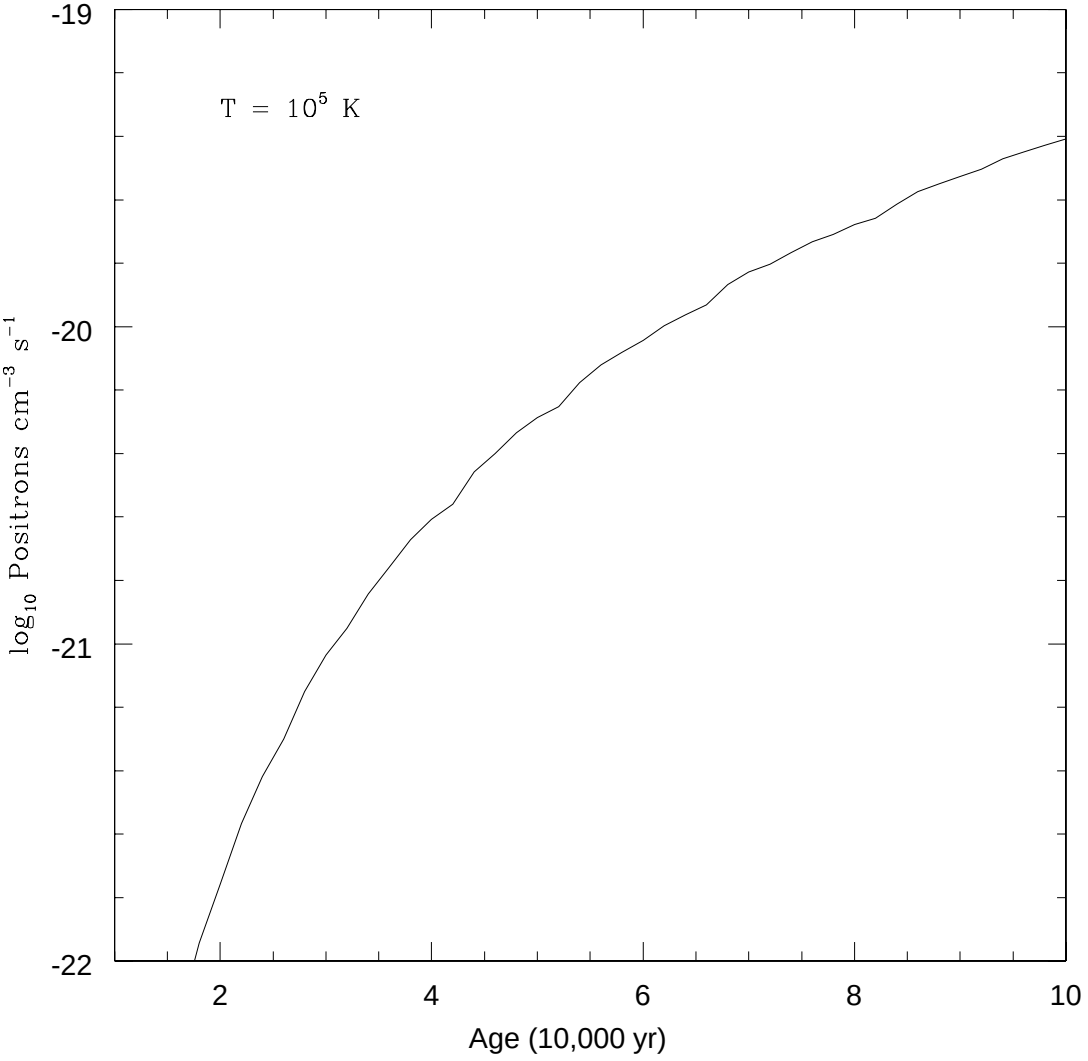

Fig. 10.— The thermalization rate as a function of age for Sgr A East.

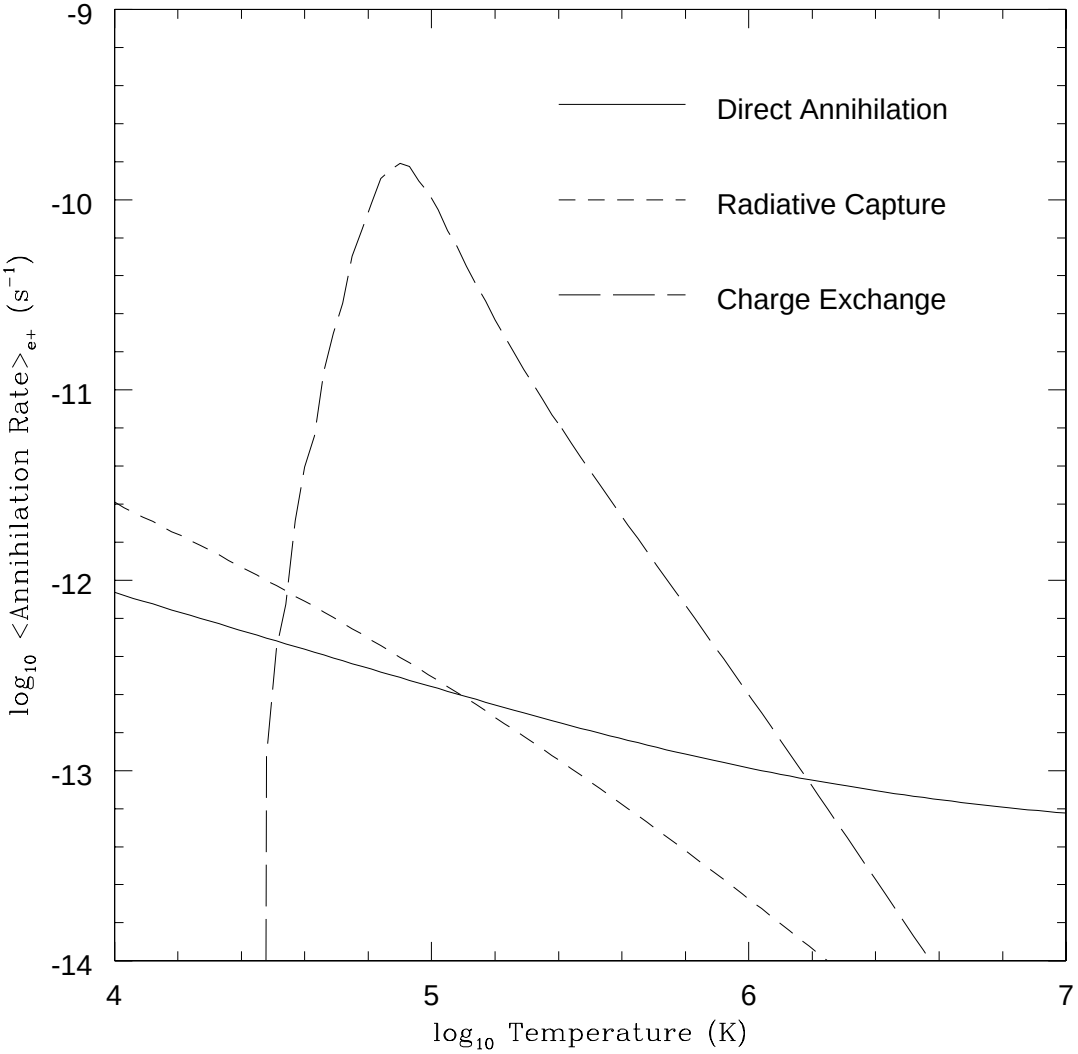

Fig. 11.— The positron annihilation rates averaged over the positron distribution as a function of temperature.

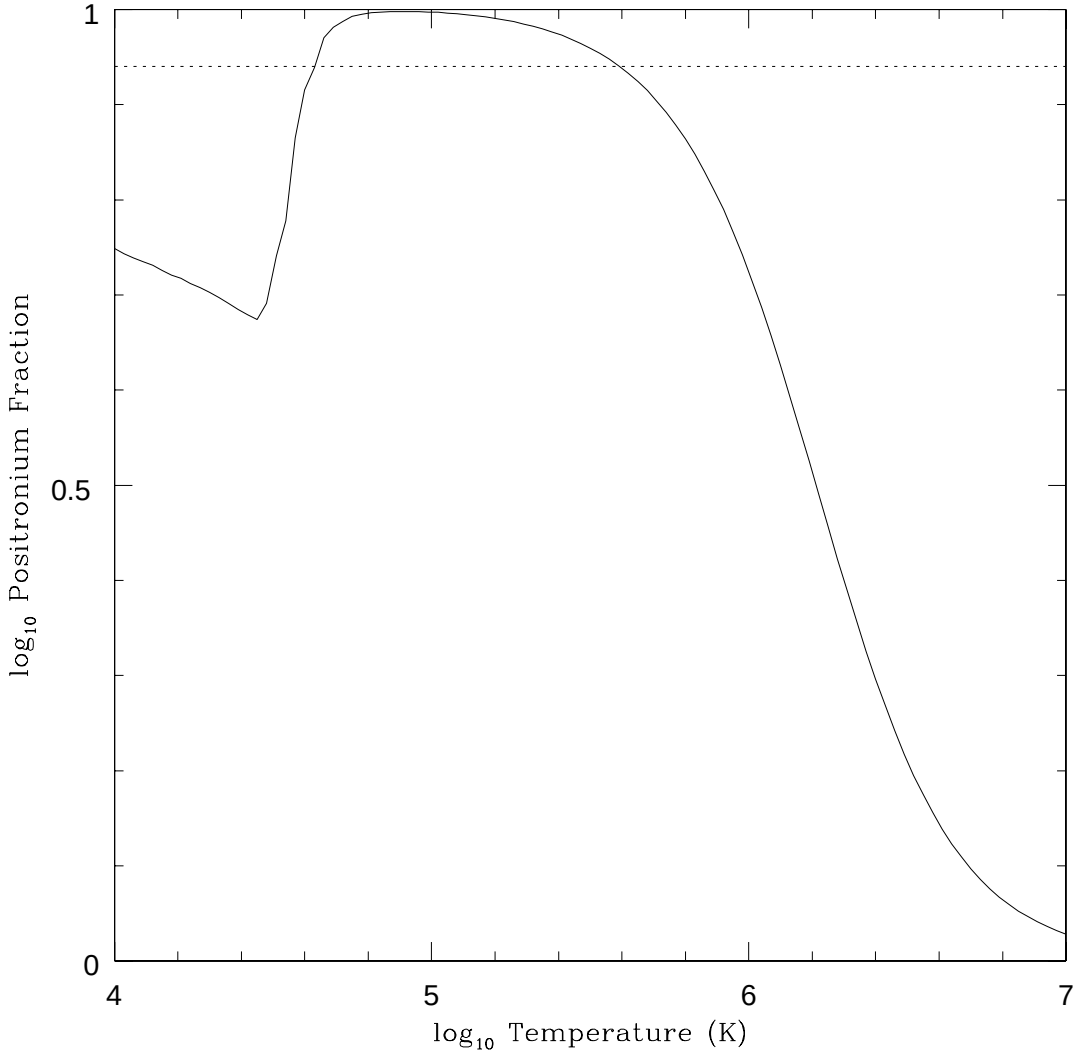

Fig. 12.— The positronium fraction as a function of temperaure.

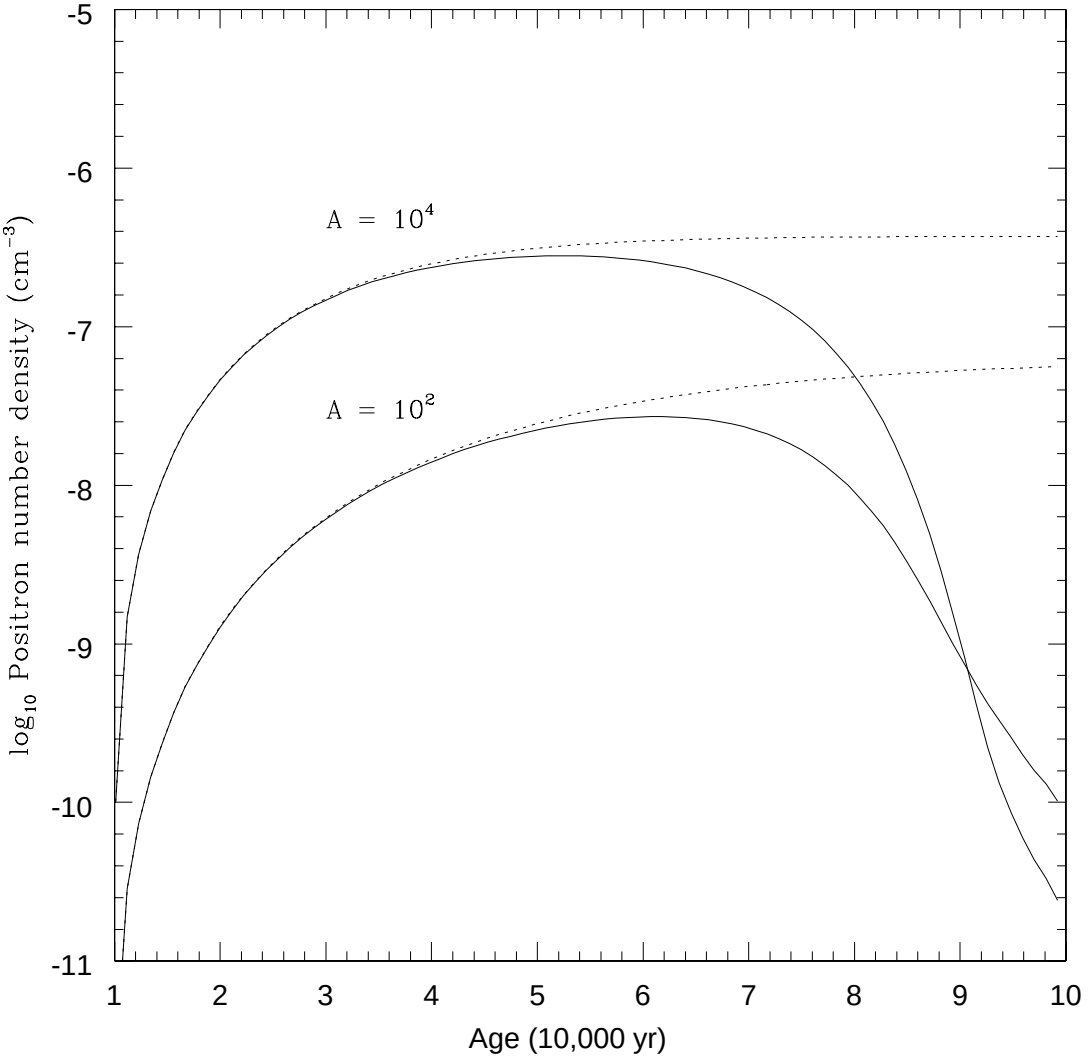

Fig. 13.— The number density of thermal positrons for the two cases considered.

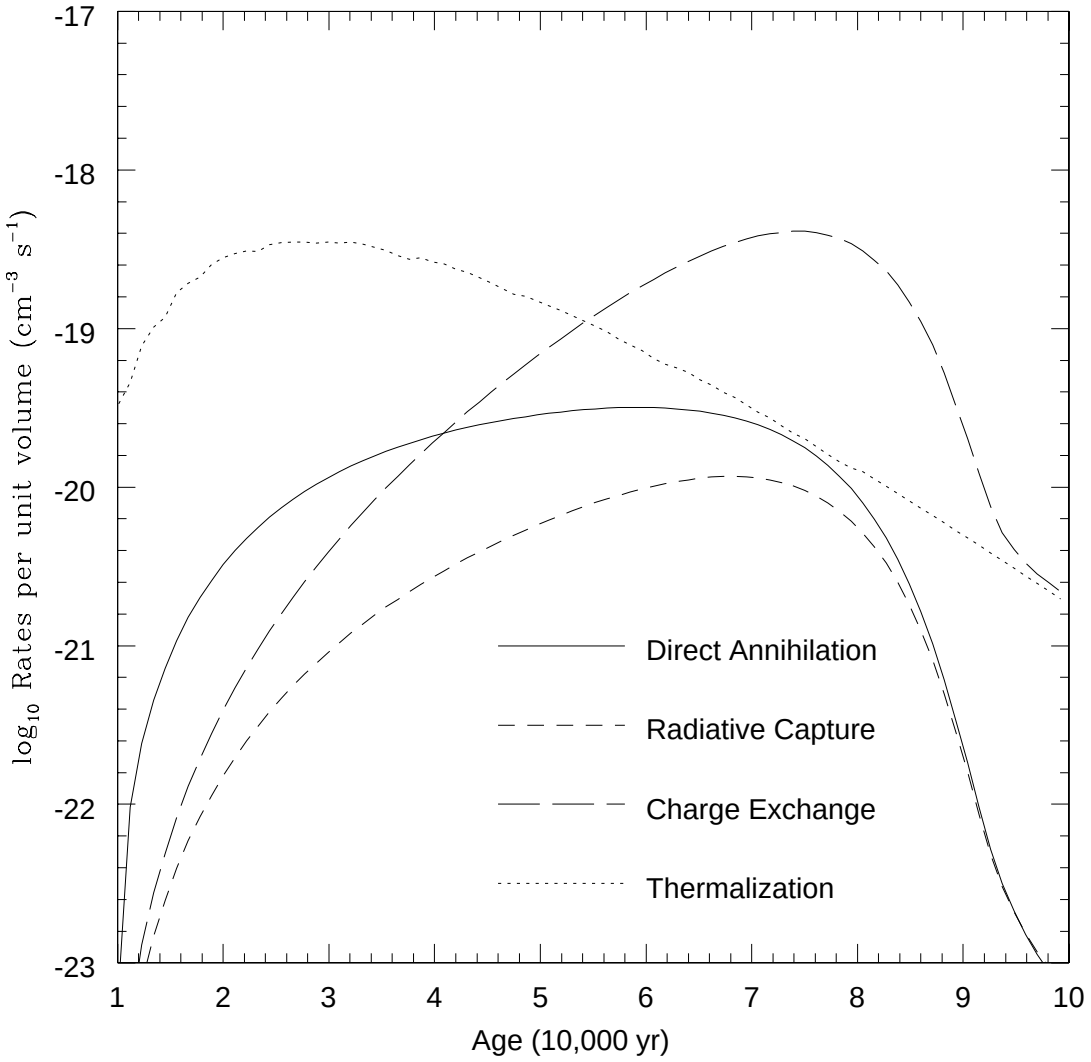

Fig. 14.— A comparison between the rates per unit volume of thermalization and annihilation as a function of age for $A = 10^4$.

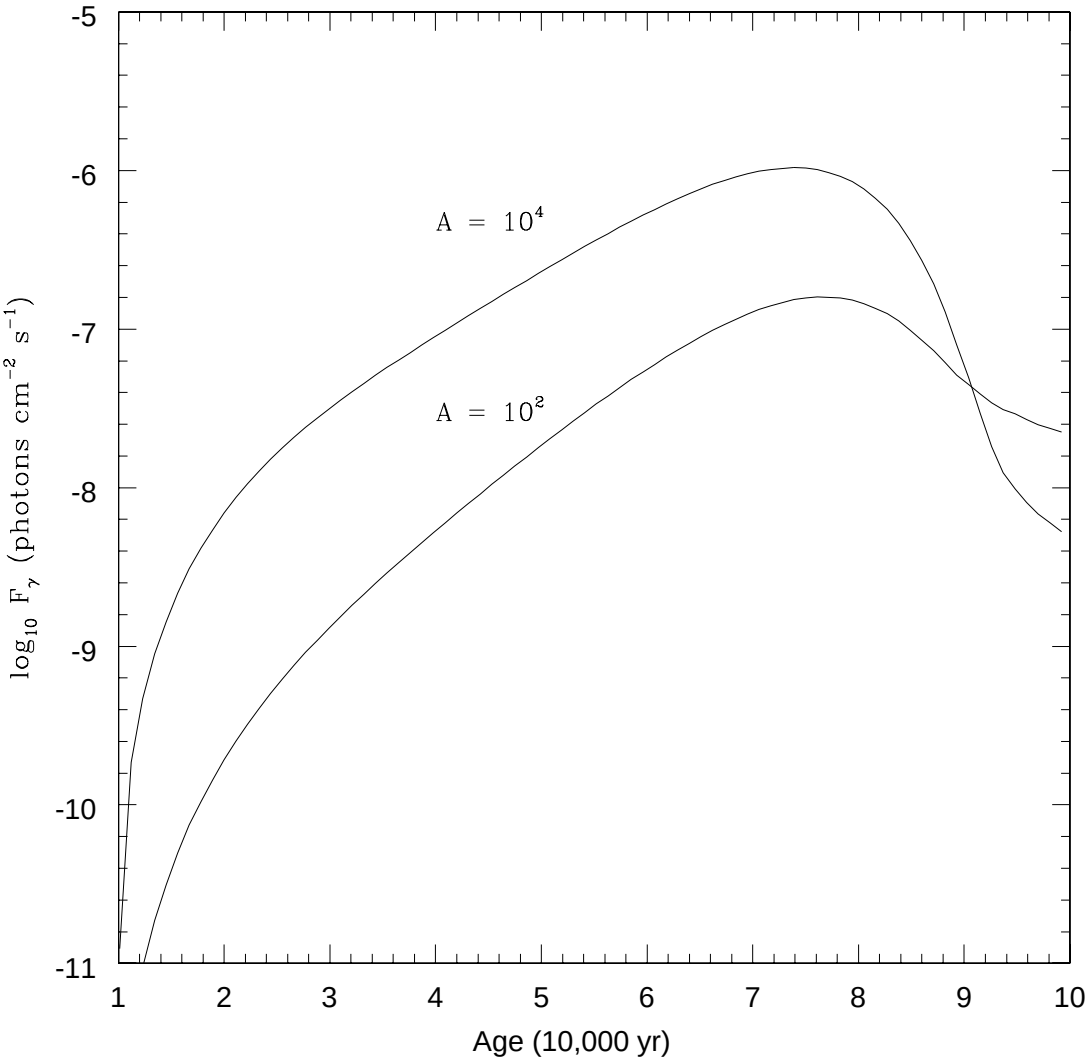

Fig. 15.— The flux (as observed at Earth) of the total number of annihilation photons for both $A = 10^2$ and $A = 10^4$ as a function of the age of Sgr A East. The flux peaks shortly after the annihilation rate due to charge exchange exceeds the thermalization rate (see Figure 14).

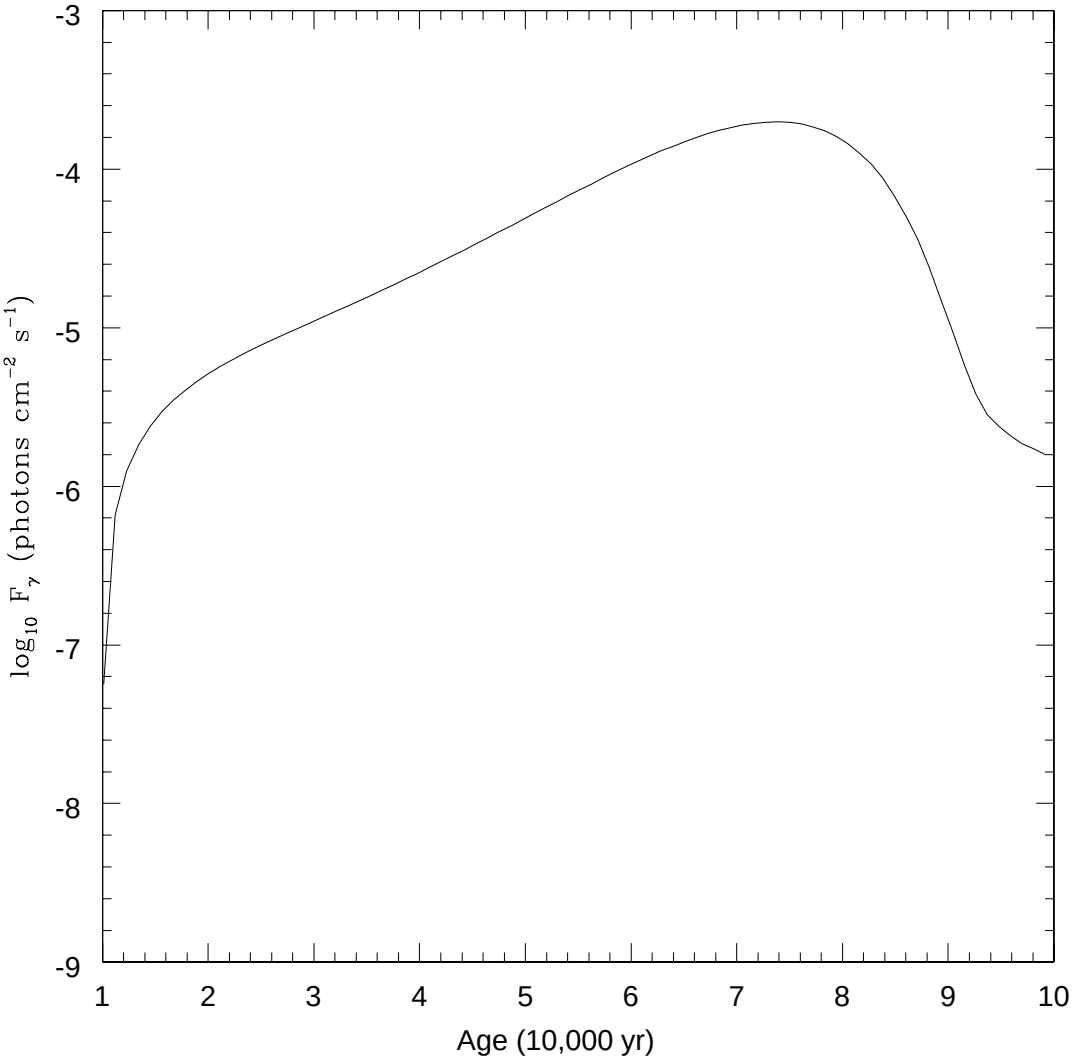

Fig. 16.— The flux as observed on Earth of the total number of annihilation photons for $A = 10^2$ under the *ad hoc* assumption that all injected positrons thermalize on a time scale that is much shorter than the age of Sgr A East.